International Journal of Geo-Information

MDPI

Article

Urban–Rural Exposure to Flood Hazard and Social Vulnerability in the Conterminous United States

Bishal Dhungana and Weibo Liu *

Department of Geosciences, Florida Atlantic University, Boca Raton, FL 33431, USA; bdhungana2023@fau.edu
* Correspondence: liuw@fau.edu; Tel.: +1-561-297-4965

Abstract: This study investigates the spatial disparities in flood risk and social vulnerability across 66,543 census tracts in the Conterminous United States (CONUS), emphasizing urban–rural differences. Utilizing the American Community Survey (ACS) 2016–2020 data, we focused on 16 social factors representing socioeconomic status, household composition, racial and ethnic minority status, and housing and transportation access. Principal Component Analysis (PCA) reduced these variables into five principal components: Socioeconomic Disadvantage, Elderly and Disability, Housing Density and Vehicle Access, Youth and Mobile Housing, and Group Quarters and Unemployment. An additive model created a comprehensive Social Vulnerability Index (SVI). Statistical analysis, including the Mann–Whitney U test, indicated significant differences in flood risk and social vulnerability between urban and rural areas. Spatial cluster analysis using Local Indicators of Spatial Association (LISA) revealed significant high flood risk and social vulnerability clusters, particularly in urban regions along the Gulf Coast, Atlantic Seaboard, and Mississippi River. Global and local regression models, including Ordinary Least Squares (OLS) and Geographically Weighted Regression (GWR), highlighted social vulnerability's spatial variability and localized impacts on flood risk. The results showed substantial regional disparities, with urban areas exhibiting higher flood risks and social vulnerability, especially in southeastern urban centers. The analysis also revealed that Socioeconomic Disadvantage, Group Quarters and Unemployment, and Housing Density and Vehicle Access are closely related to flood risk in urban areas, while in rural areas, the relationship between flood risk and factors such as Elderly and Disability and Youth and Mobile Housing is more pronounced. This study underscores the necessity for targeted, region-specific strategies to mitigate flood risks and enhance resilience, particularly in areas where high flood risk and social vulnerability converge. These findings provide critical insights for policymakers and planners aiming to address environmental justice and promote equitable flood risk management across diverse geographic settings.

Keywords: flood risk; social vulnerability; geographically weighted regression; urban–rural

check for updates

Citation: Dhungana, B.; Liu, W. Urban–Rural Exposure to Flood Hazard and Social Vulnerability in the Conterminous United States. *ISPRS Int. J. Geo-Inf.* **2024**, *13*, 339. https://doi.org/10.3390/ijgi13090339

Academic Editors: Wolfgang Kainz, Dimitrios D. Alexakis and Adrianos Retalis

Received: 9 July 2024
Revised: 15 September 2024
Accepted: 16 September 2024
Published: 22 September 2024

Copyright: © 2024 by the authors. Published by MDPI on behalf of the International Society for Photogrammetry and Remote Sensing. Licensee MDPI, Basel, Switzerland. This article is an open access article distributed under the terms and conditions of the Creative Commons Attribution (CC BY) license (https://creativecommons.org/licenses/by/4.0/).

1. Introduction

Flooding poses a significant and frequent threat in the United States (US), causing extensive damages to infrastructure, property, and human lives. The escalating frequency and intensity of flood events, exacerbated by climate change, have heightened risks across diverse geographic regions of the Conterminous United States (CONUS). Coastal areas face threats from storm surges and rising sea levels, while riverine and inland regions are susceptible to river floods and flash floods triggered by heavy rainfall [1,2]. According to the US Geological Survey (USGS) Fact Sheet 2006–3026, flood is the most recurrent natural disaster in the US, which on average causes the deaths of about 140 people and property damage worth USD 6 billion each year [3]. Recent studies highlight an increasing prevalence of extreme precipitation events, further intensifying flood hazards nationwide [4,5]. The Federal Emergency Management Agency (FEMA) underscores floods' economic and human toll, affecting millions of Americans annually through displacement and property damage [6].

Social vulnerability is a crucial component of environmental justice, representing the capacity of social groups to predict, manage, withstand, and recover from environmental hazards [7]. The vulnerability is shaped by socioeconomic factors such as income, race, education level, and housing status. Individuals with lower incomes frequently lack health insurance and are less likely to own homes or vehicles, which heightens their social vulnerability [8]. The Social Vulnerability Index (SVI), developed by CDC/ATSDR, assesses administrative-level vulnerability using indicators such as socioeconomic status, household composition, and access to resources [9]. Social vulnerability exacerbates flood impacts, disproportionately affecting racial minorities and low-income groups which are concentrated in high-risk flood zones [7,10,11]. These populations face compounded challenges due to socioeconomic disparities, hindering their access to resources and resilience against environmental hazards [12–14]. Studies [15–17] document significant disparities in flood risk, revealing that minority and lower-socioeconomic-status households often experience more severe flooding and delayed recovery, particularly evident during events like Hurricane Harvey. The lack of social, financial, and political support structures cause this type of disparity [17].

A study in Canada emphasized integrating social vulnerability and flood risk to develop equitable flood management policies, highlighting higher risks among vulnerable groups like Indigenous peoples and economically insecure residents [18]. In the US, poor populations are more likely to live in flood-prone areas, especially in inland regions, where limited resources exacerbate their vulnerability to flood risks [14,19]. The intersection of social vulnerability and flood risk underscores the necessity for comprehensive and equitable flood risk management strategies. These strategies must address disadvantaged communities' specific needs and vulnerabilities and promote social equity and environmental justice in flood risk mitigation efforts [7,15,16]. The relationship between vulnerability and flood risk is, however, much more complex. For instance, it has been found that in Miami, Florida, socially privileged groups expose themselves to flood risks for coastal amenities, while in Houston, Texas, socially vulnerable people predominantly inhabit flood zones due to petrochemical industries making coastal areas less desirable to wealthier populations [20]. This suggests that vulnerable groups may face higher risks, while advantaged groups often reside in flood-prone areas for amenities, reflecting unequal resource access and power dynamics. It is therefore important to conduct a more in-depth analysis, considering all the geographical, socioeconomic, and geopolitical factors while dealing with social vulnerability to flood.

While urban flooding poses a significant and escalating threat, disproportionately affecting marginalized communities, the focus on urban areas often neglects the distinct vulnerabilities and mitigation needs of rural regions [21]. Climate change exacerbates the frequency and severity of urban floods, impacting densely populated areas with extensive infrastructure [21]. Urban areas, particularly those situated along coasts and rivers, typically face elevated flood risks exacerbated by dense populations, extensive infrastructure, and heightened social vulnerability among socioeconomically disadvantaged communities [12]. Studies underscore pronounced disparities in flood risk along racial, ethnic, and socioeconomic lines in major cities like Miami and Houston, emphasizing environmental justice concerns [22]. Conversely, rural areas may face lower overall flood risk, yet they often contend with substantial social vulnerability stemming from economic disadvantages and limited access to resources [12]. Moreover, these communities, reliant on urban centers for essential services, encounter distinct hurdles in flood risk mitigation, exacerbated by inadequate resources and uneven funding allocations [23]. This is evident in regions like the southeastern US, where socially vulnerable counties receive less Flood Mitigation Assistance (FMA) funding despite greater needs [24]. Integrating spatially heterogeneous analyses is essential for understanding rural vulnerabilities and developing tailored flood management strategies that address local socioeconomic and environmental dynamics [25,26]. Advanced methodologies like AI and hydrodynamic models offer promising tools for enhancing flood susceptibility mapping but are underuti-

lized in rural contexts [27]. Therefore, addressing the inequitable distribution of resources and bridging the urban–rural divide in flood vulnerability assessments are essential for fostering equitable resilience across diverse geographic landscapes.

Previous studies have utilized different types of spatial and statistical approaches to analyze the relationship between vulnerability and flood hazard. Univariate and bivariate Local Indicators of Spatial Association (LISA) have provided national and regional clusters of vulnerability and flood hazard [13–15,19]. Research using methodologies like Geographically Weighted Regression (GWR) and Multiscale Geographically Weighted Regression (MGWR) has demonstrated the importance of capturing local variations in flood risk and social vulnerability, highlighting the need for region-specific strategies [12]. The use of GWR models has revealed significant local variations in flood risk and social vulnerability, underscoring the need for detailed, localized analyses to inform flood risk management strategies [12]. This can be further supported by a recent study in Canada which underscored the significance of GWR in elucidating spatial heterogeneity and environmental injustices in flood hazard exposure [10]. This study addresses the need for a detailed analysis of urban–rural disparities in flood exposure and social vulnerability across the CONUS. It aims to provide a comprehensive understanding of how different areas are affected by flood risks, considering socioeconomic and geographic factors. Employing advanced spatial analysis methods, including LISA and GWR, we aim to identify and analyze significant patterns of flood exposure and social vulnerability at a detailed and localized level. This study highlights different communities' challenges and disparities by focusing on urban and rural settings, ultimately informing more effective and equitable flood risk management strategies.

2. Materials and Methods

2.1. Study Area

The CONUS, consisting of the 48 adjoining states and the District of Columbia, is selected for a comprehensive study on flood hazards due to its extensive flood data availability and diverse geographic features. This selection is crucial as it includes urban centers, coastal areas, riverine environments, and isolated locales, representing the multifaceted nature of flood risks and community vulnerabilities. Census tracts, averaging about 4000 inhabitants, are small, relatively permanent subdivisions of a county designed for homogeneous population characteristics. The 2020 census tracts form the basis of this study, providing updated and detailed demographic and geographic data. This granularity facilitates a precise analysis of localized flood impacts, making census tracts ideal for flood hazard studies. Our focus is on 66,543 out of 83,509 census tracts within the CONUS that have experienced flooding and for which complete data exist.

2.2. Floodplain Data

FEMA's National Flood Insurance Program (NFIP) plays a pivotal role in flood risk management by creating Flood Insurance Rate Maps (FIRMs) that delineate the Special Flood Hazard Area (SFHA), highlighting the 100-year floodplain with a 1% annual chance of flooding. However, due to economic, political, and geographical factors, a significant portion of the CONUS—mainly rural and less developed regions—remains unmapped, posing a substantial gap in flood risk management and land use planning [28]. A Random Forest (RF) classification technique was used to address this gap, and a 100-year, 30-meter-resolution flood inundation layer was developed for the entire CONUS. It was achieved using FEMA SFHA maps and ten predictive variables for each Hydrologic Unit Code level four (HUC-4) region [28]. The floodplain data were sourced from the US Environmental Protection Agency's (EPA) EnviroAtlas website "https://www.epa.gov/enviroatlas/enviroatlas-interactive-map (accessed on 15 September 2023)". The ArcGIS Pro statistics tool, in conjunction with the flood raster layer, facilitated the calculation of the flooded zone area for each census tract. Figure 1 shows the distribution of flooded zone area percentage of each census tract used in our analysis.

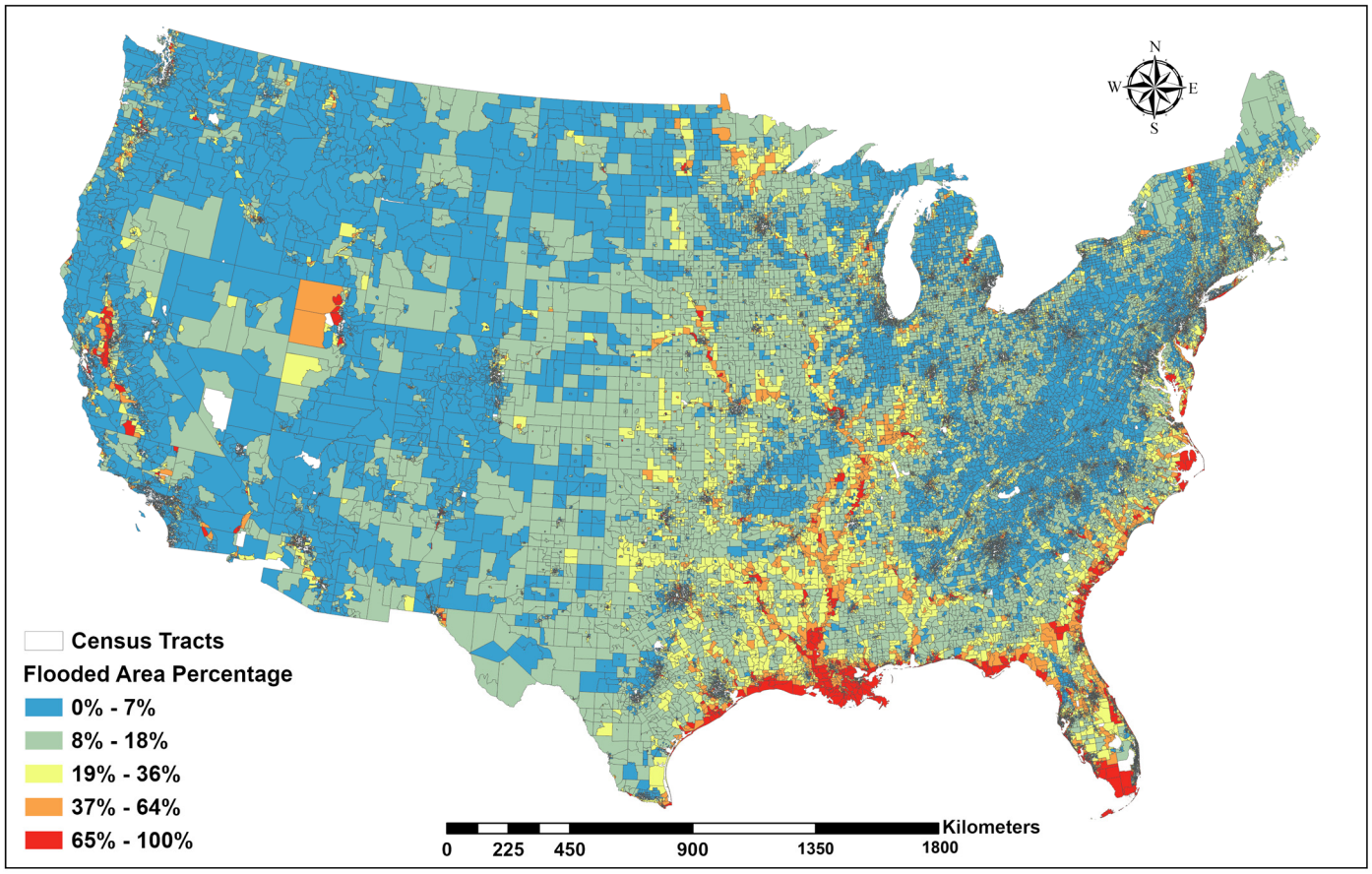


Figure 1. Distribution of flooded zone area percentage in each census tract.

2.3. Urban–Rural Classification

The Rural–Urban Commuting Area (RUCA) codes are a classification system developed by the US Department of Agriculture to categorize US census tracts for a detailed and nuanced understanding of the rural–urban continuum in the US, reflecting variations in population density, proximity to the Metropolitan Statistical Area (MSA), and commuting behaviors [29,30]. These RUCA codes, which contain primary and secondary codes, were revised on 7 March 2019. These RUCA codes are available for the census tracts based on the 2010 census division. Using the census tract relationship files between 2010 and 2020 provided by the US Census Bureau, the RUCA categories were merged with the 2020 census tract attribute table [31].

For our analysis, the ten primary RUCA categories, as shown in Table 1, were subdivided into two categories (urban and rural). Among the 66,543 census tracts considered for our analysis, 51,990 are considered urban tracts (metro), and the remaining 14,553 are rural tracts (non-metro). The reclassified census tract distribution is shown in Figure 2.

Table 1. Division of RUCA primary codes into two categories.

Urban Areas	Rural Areas
Metropolitan area core (RUCA = 1)	Micropolitan area core (RUCA = 4)
Metropolitan area high commuting (RUCA = 2)	Micropolitan area high commuting (RUCA = 5)
Metropolitan area low commuting (RUCA = 3)	Micropolitan area low commuting (RUCA = 6)
	Small town core (RUCA = 7)
	Small town high commuting (RUCA = 8)
	Small town low commuting (RUCA = 9)
	Rural (RUCA = 10)

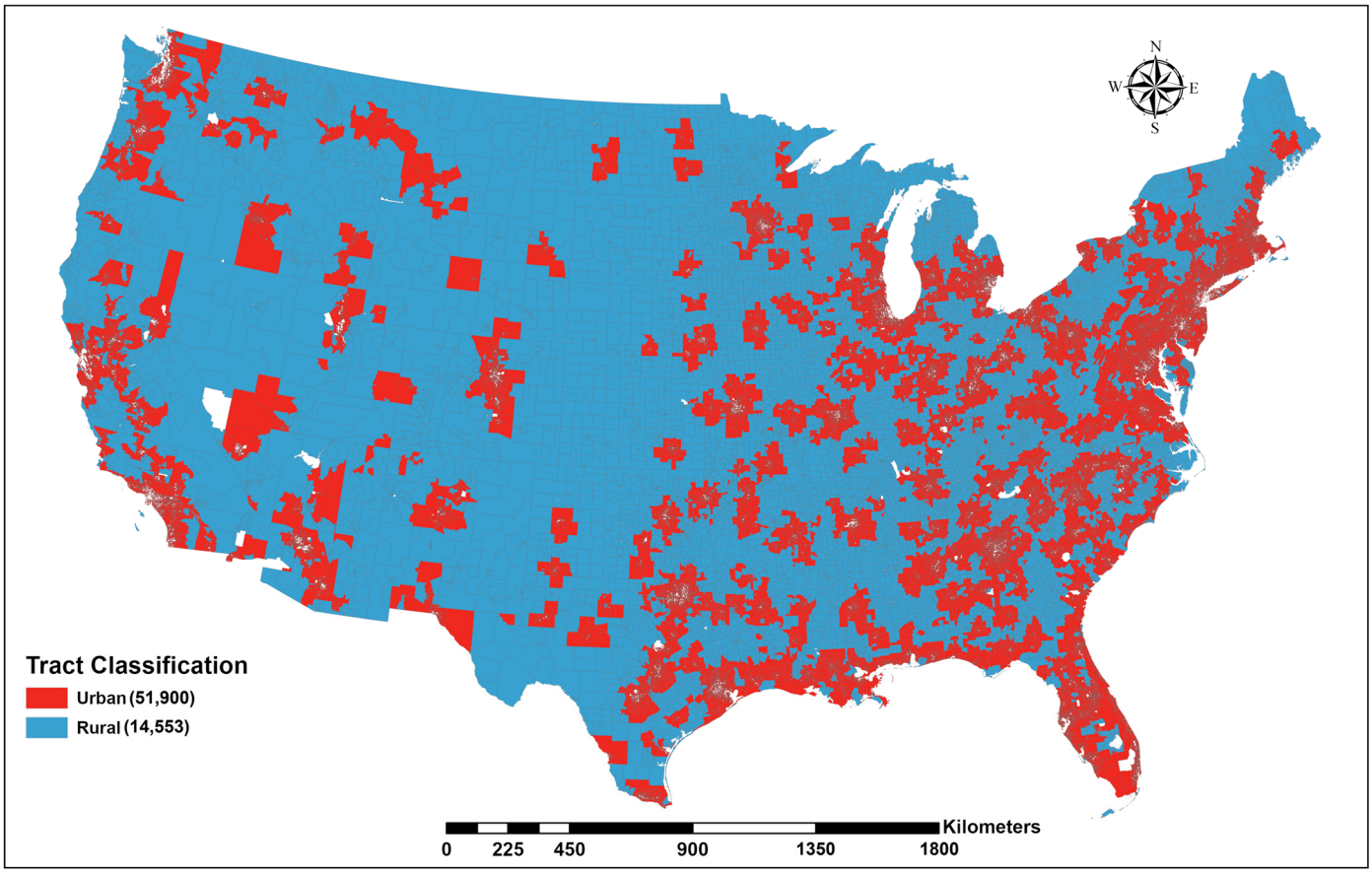


Figure 2. Reclassified census tracts into urban–rural categories.

2.4. Social Vulnerability Variables

We utilized data from the American Community Survey (ACS) 2016–2020, focusing on 16 social vulnerability factors. These variables encompass socioeconomic status, household composition, racial and ethnic minority status, and housing and transportation access, as listed in Table 2. The data cover 84,122 census tracts across the US, with the dataset available in multiple formats, including CSV and Esri Geodatabase from the CDC/ATSDR SVI database. The Esri Geodatabase was from https://www.atsdr.cdc.gov/placeandhealth/svi/data_documentation_download.html (accessed on 15 September 2023), and only 66,543 tracts were filtered as required for our analysis.

Table 2. Variables used for the construction of SVI.

Variables	Description
E_POV150	Persons below 150% poverty estimate, 2016–2020 ACS
E_UNEMP	Civilians (age 16+) unemployed estimate, 2016–2020 ACS
E_HBURD	Housing cost-burdened occupied housing units with annual income less than USD 75,000 (30%+ of income spent on housing costs) estimate, 2016–2020 ACS
E_NOHSDP	Persons (age 25+) with no high school diploma estimate, 2016–2020 ACS
E_UNINSUR	Uninsured in the total civilian noninstitutionalized population estimate, 2016–2020 ACS
E_AGE65	Persons aged 65 and older estimate, 2016–2020 ACS
E_AGE17	Persons aged 17 and younger estimate, 2016–2020 ACS
E_DISABL	Civilian noninstitutionalized population with a disability estimate, 2016–2020 ACS
E_SNGPNT	Single-parent household with children under 18 estimate, 2016–2020 ACS
E_LIMENG	Persons (age 5+) who speak English “less than well” estimate, 2016–2020 ACS

Table 2. *Cont.*

Variables	Description
E_MINRTY	Minority (Hispanic or Latino (of any race); Black and African American, Not Hispanic or Latino; American Indian and Alaska Native, Not Hispanic or Latino; Asian, Not Hispanic or Latino; Native Hawaiian and Other Pacific Islander, Not Hispanic or Latino; Two or More Races, Not Hispanic or Latino; Other Races, Not Hispanic or Latino) estimate, 2016–2020 ACS
E_MUNIT	Housing in structures with 10 or more units estimate, 2016–2020 ACS
E_MOBILE	Mobile homes estimate, 2016–2020 ACS
E_CROWD	At household level (occupied housing units), more people than rooms estimate, 2016–2020 ACS
E_NOVEH	Households with no vehicle available estimate, 2016–2020 ACS
E_GROUPQ	Persons in group quarters estimate, 2016–2020 ACS

2.5. SVI Construction

After data preprocessing, which involved standardizing the 16 variables, Principal Component Analysis (PCA) was performed to reduce the number of variables. This data reduction technique provides a robust and consistent set of variables, facilitates data reproduction, and simplifies data compilation [7]. The PCA was performed using the "sklearn" Python module [32], and the selection of components was based on eigenvalues greater than 1.0, following the Kaiser criterion [33]. The analysis identified 5 principal components from the original 16 sub-categories, which explained about 72% variance in the dataset. The principal components were named according to their leading variables; however, each component consisted of multiple variables contributing to its overall structure. This naming serves as a simplification of the underlying complexity. Table 3 summarizes the identified components, the percentage of variance explained, and the dominant variables.

Table 3. Identified components from PCA and dominant variables.

Component Number	Component Name	Percentage of Variation Explained (%)	Dominant Variable	Correlation
1	Socioeconomic Disadvantage	35.58	E_POV150	0.80
2	Elderly and Disability	11.14	E_AGE65	0.79
3	Housing Density and Vehicle Access	10.91	E_MUNIT	0.81
4	Youth and Mobile Housing	7.25	E_AGE17	0.76
5	Group Quarters and Unemployment	6.49	E_GROUPQ	0.64

To create a comprehensive SVI for each census tract, an additive model combined the five components into a single measure, assuming each component is equally essential and carries equal weight. This additive approach aligns with previous research [7] and is considered the best method to integrate multidimensional components into a singular measure [34]. The direction of each component was adjusted so that all components positively contribute to the overall vulnerability, ensuring that higher SVI values consistently indicate greater vulnerability across the CONUS.

2.6. Statistical Analysis

The flooded zone area value of each tract was skewed to the right, so it was log-transformed (log10(x)) to improve data normality. Census tracts were classified as urban (1) or rural (0) to create a location variable. To examine differences between these locations, the Mann–Whitney U two-sample *t*-test was applied to the log-transformed flooded zone area, and the overall SVI was calculated by additive aggregation of the principal compo-

nents to identify statistically significant differences in mean ranks between urban and rural tracts [35].

Before delving into advanced spatial analysis techniques, it is crucial to identify and understand spatial patterns in the data. Cluster analysis methods, such as LISA, were utilized to detect spatial clusters and hotspots of social vulnerability and flood risk [36]. LISA helps identify areas with significant local spatial autocorrelation, essential in understanding the geographic distribution of vulnerable populations and areas prone to flooding. This step ensures that the spatial characteristics of the data are well understood, which is critical for subsequent analysis.

Global models, such as the Ordinary Least Squares (OLS) linear regression, were initially used to check for the significance of relationships between the dependent variable (flooded zone area) and independent variables (SVI components). GWR was then employed to address spatial non-stationarity [37]. GWR is a local spatial analysis technique that allows variable relationships to vary across space, suitable for spatial non-stationarity and autocorrelation data. Using the MGWR package in Python [38], we conducted separate GWR models for urban and rural areas, as well as an overall model encompassing all tracts, to capture loc14alized impacts of environmental factors across different settings. The critical step in the GWR analysis involved using the Sel_BW function to determine the optimal bandwidth, which is crucial for adjusting the scale of analysis to the data's spatial structure, using a Gaussian adaptive bi-square kernel to manage spatial non-stationarity. Bandwidth selection is critical as it influences the resolution at which the data are analyzed, affecting the local versus global relevance of the results. With the optimal bandwidth determined, the GWR models were able to adjust relationships between variables locally, providing insights into geographic disparities in flood impacts. Model performance was evaluated using local R-squared values and the Corrected Akaike Information Criterion (AICc) to assess explanatory power and effectiveness across different regions. Finally, we used Kernel Density Estimation (KDE) plots to visualize the distribution of GWR coefficients across urban and rural areas using the equal area under the curve. KDE plots were selected for their ability to provide a smooth, continuous representation of the underlying distribution, allowing for a clear comparison between the two geographic zones.

3. Results

3.1. Spatial Distributions and Patterns

The analysis of 66,543 census tracts within the CONUS reveals significant spatial variability in flood risk, social vulnerability, and urban–rural disparities. Urban areas, especially those in coastal and riverine environments, exhibit higher flood risk compared to rural areas. The overall SVI highlights regions with high social vulnerability that often coincide with areas of significant flood risk, indicating compounded risks for socially disadvantaged communities. Based on RUCA codes, the urban–rural classification shows clear distinctions in the spatial distribution of flood risk and social vulnerability.

The examination of flood risk (Figure 1), urban–rural distribution (Figure 2), and social vulnerability (Figure 3) across the CONUS highlights notable regional disparities and areas of concern. Urban areas along the coasts and major rivers, such as the Gulf Coast, Atlantic Seaboard, and the Mississippi River, show high flood risk and varying levels of social vulnerability. Regions like the Northeast Megalopolis and urban centers in the Southeast present overlapping high flood risks and social vulnerability, indicating potential hotspots of environmental injustice. Conversely, rural areas in the central and western CONUS, including the Great Plains and Appalachian regions, face lower overall flood risk but still experience significant social vulnerability, particularly among socioeconomically disadvantaged communities. Transition zones between urban and rural areas exhibit a mixed risk profile, necessitating nuanced policy interventions that address urban infrastructure needs and rural resource limitations. These findings underscore the necessity for targeted, region-specific strategies to mitigate flood risks and enhance resilience, particularly in areas where high flood risk and social vulnerability converge.

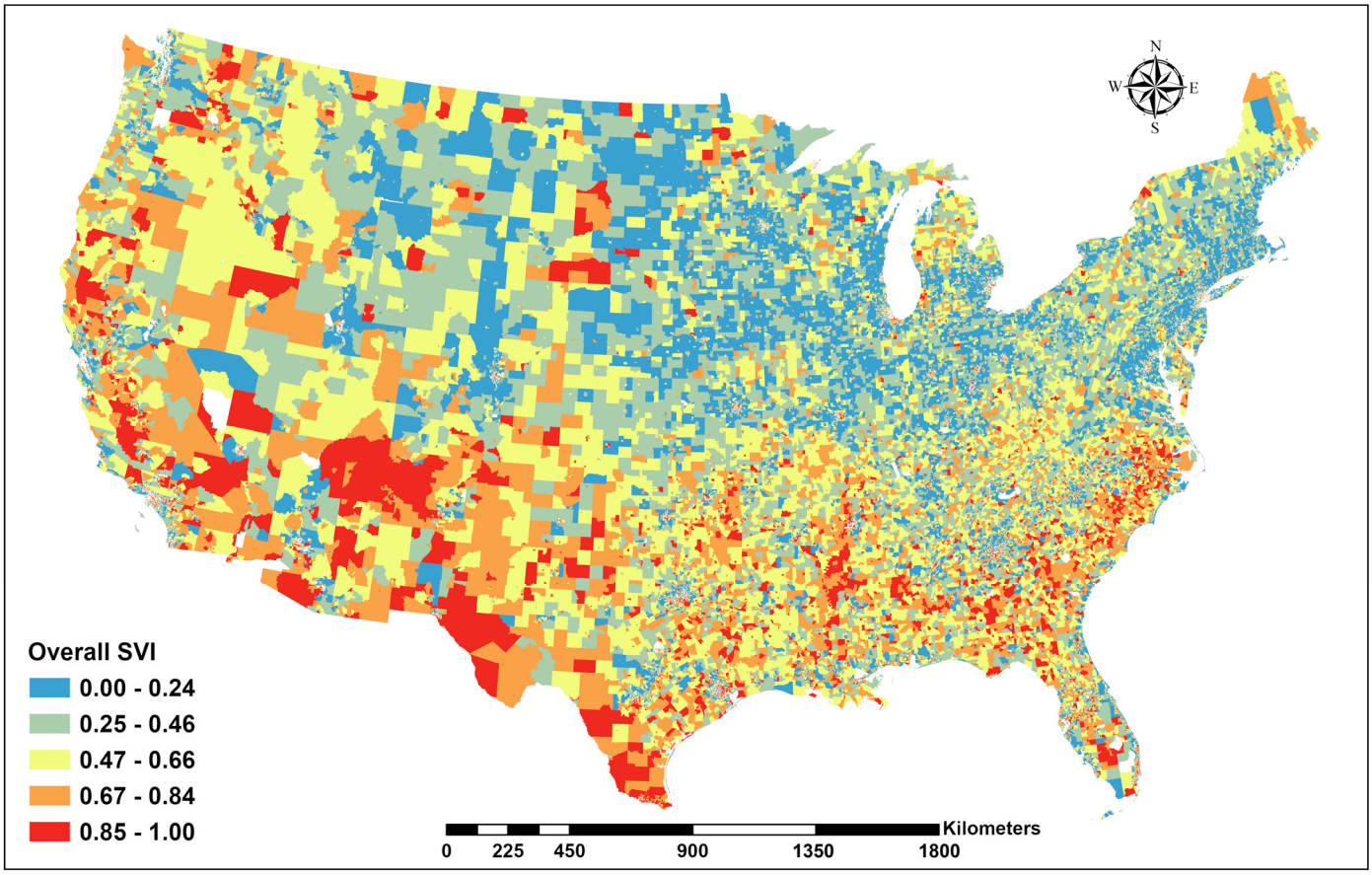


Figure 3. The SVI at the census tract level for the CONUS.

The Mann–Whitney U two-sample *t*-test results indicate significant differences in flood risk and social vulnerability between urban and rural census tracts in the CONUS. Specifically, the overall SVI and the log-transformed flooded zone area show highly significant differences, with *p*-values ($p < 0.01$) indicating that these disparities are not due to random chance. Each of the principal components of social vulnerability also exhibits significant differences between urban and rural areas.

Figures 4 and 5 illustrate the statistically significant (at the 95% confidence interval) hot spots, cold spots, and spatial outliers of flood risk and social vulnerability. Notably, overlaps between the significant clusters of high flood risk and high social vulnerability indicate areas of compounded risk. For instance, significant hot spots of both flood risk and high social vulnerability are found in the southeastern US, particularly along the Gulf Coast and parts of the Mississippi River basin. The LISA analysis for the SVI reveals notable differences between urban and rural areas. High–high clusters, which indicate areas of high social vulnerability surrounded by similarly vulnerable tracts, are predominantly found in urban regions, with 12,416 urban tracts compared to 3752 rural tracts. This pattern highlights significant pockets of social vulnerability within urban centers, particularly in the southeastern US and along the Mississippi River Basin. Conversely, low–low clusters, representing areas of low social vulnerability, are also more common in urban areas (13,547 tracts) than rural areas (1364 tracts), predominantly in the northwestern US.

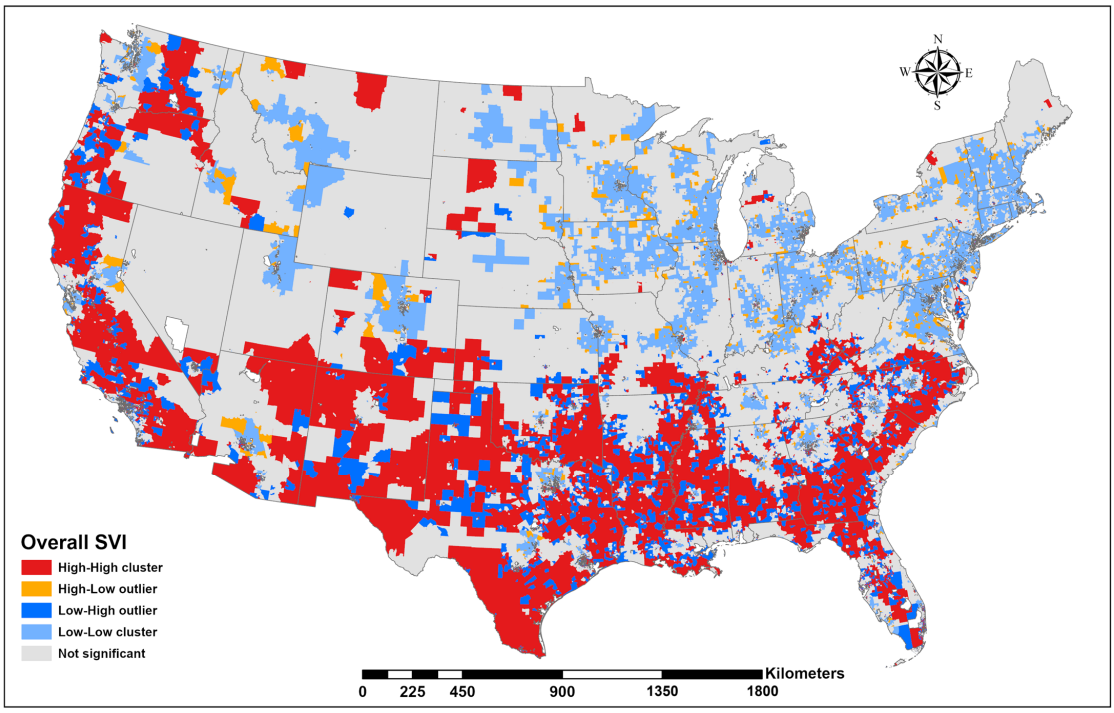


Figure 4. Clusters of the overall SVI.

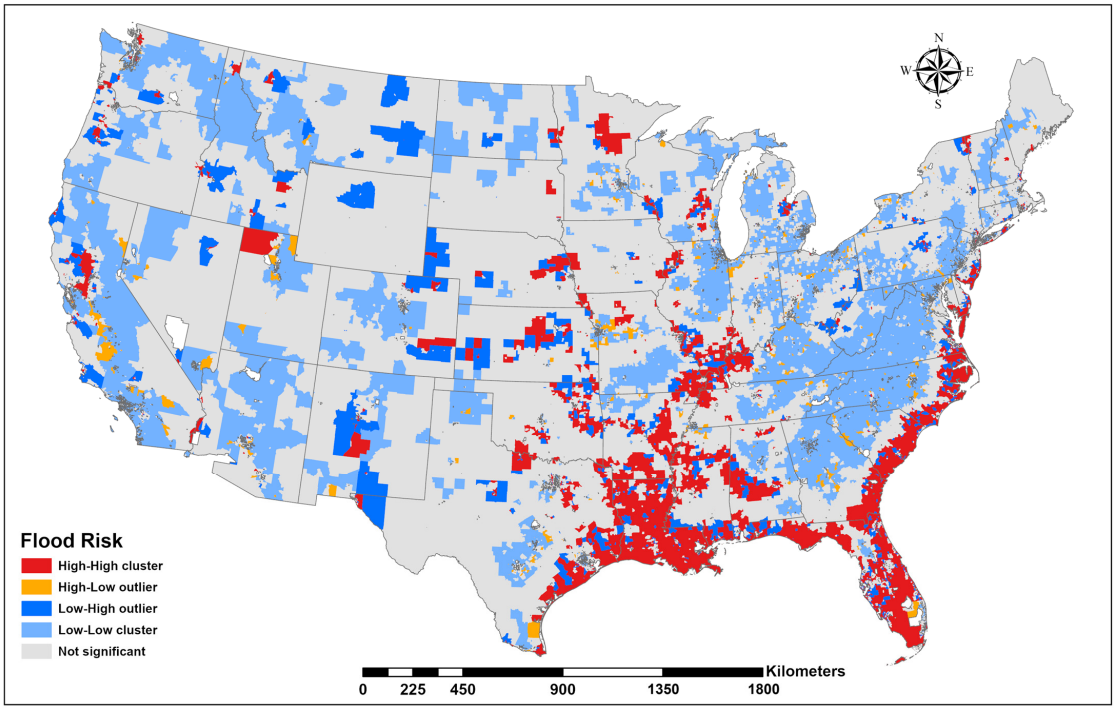


Figure 5. Clusters of flood risk.

On the other hand, flood risk mirrors the patterns observed for social vulnerability, with urban areas again showing more significant spatial heterogeneity. High–high clusters of flood risk, indicating areas with high flood risk surrounded by similarly high-risk tracts, are more prevalent in urban areas, with 5388 urban tracts compared to 1551 rural tracts. These clusters are primarily located along the Gulf Coast and in the southeastern US, regions known for their susceptibility to flooding. Low–low clusters, representing areas with low flood risk, are also predominantly found in urban areas (19,480 tracts) compared

to rural areas (3499 tracts), particularly in the northwestern US. High–low and low–high clusters in urban areas indicate localized pockets of high flood risk within generally lower-risk regions and areas of low flood risk amidst higher-risk surroundings. This negative spatial autocorrelation may be influenced by localized topographical variations, where areas of high relief create adjacent zones of contrasting flood risk, even within urban settings, explaining the proximity of high-risk clusters to low-risk areas.

The LISA analysis of social vulnerability components (Figure 6) reveals significant spatial disparities between urban and rural areas in the CONUS. Urban areas show a higher concentration of high–high clusters for all components. These clusters, particularly prevalent in the southeastern US and major urban centers like the Northeast and California, indicate regions where poverty, elderly populations, dense housing, youth populations, and group quarters with high unemployment are concentrated. This underscores the need for targeted economic interventions, social programs, healthcare, infrastructure improvements, and support services in urban centers to address these vulnerabilities. Conversely, while exhibiting fewer high–high clusters, rural areas still show significant pockets of vulnerability with a more dispersed pattern, suggesting the need for focused support to address socioeconomic disadvantages, elderly care, housing, youth needs, and employment opportunities. These findings highlight the importance of region-specific strategies to enhance resilience and promote environmental justice in urban and rural communities.

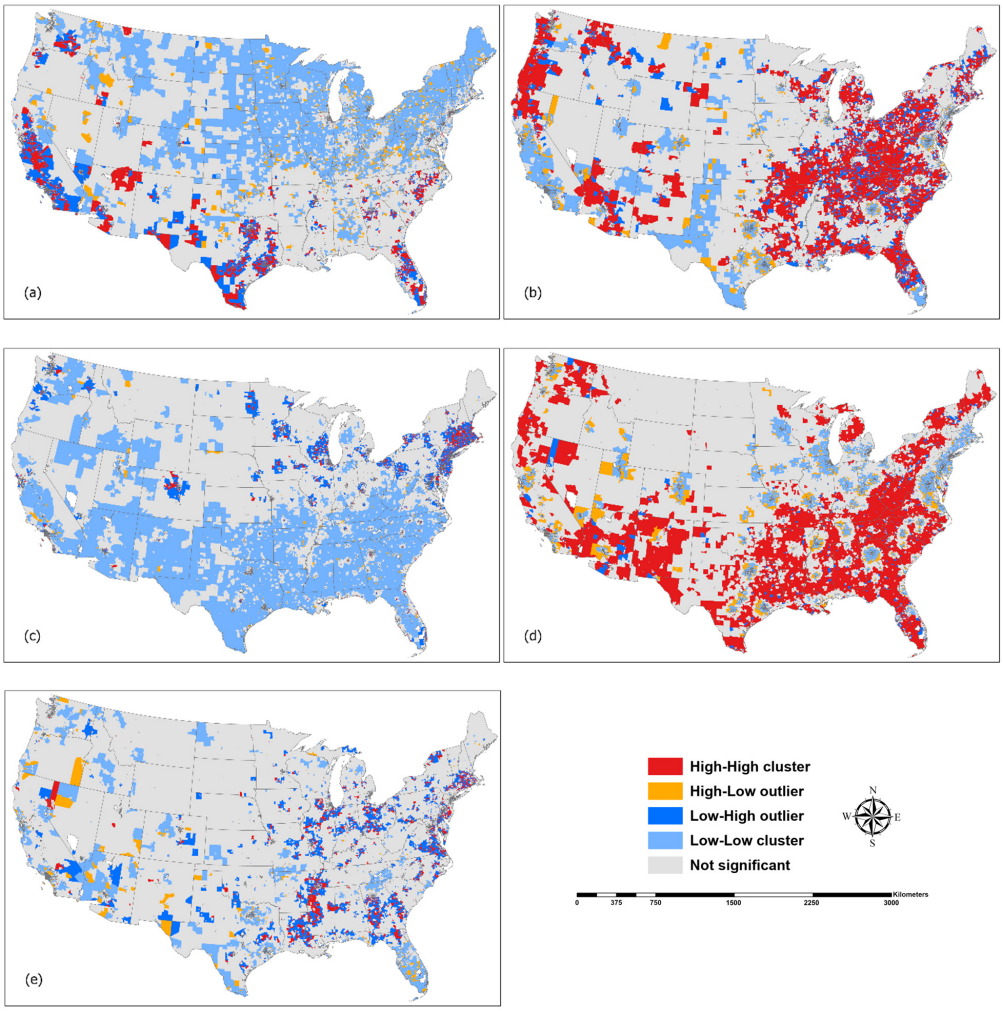


Figure 6. Clusters of hot and cold spots of (**a**) Socioeconomic Disadvantage, (**b**) Elderly and Disability, (**c**) Housing Density and Vehicle Access, (**d**) Youth and Mobile Housing, and (**e**) Group Quarters and Unemployment.

3.2. Regression Models and Spatial Variability

Table 4 compares the global OLS and the local GWR models for overall, urban (metro), and rural (non-metro) census tracts. The comparison highlights the strengths and limitations of each approach. The models were applied to the overall dataset (n = 66,543) as well as to subsets of urban (n = 51,990) and rural (n = 14,553) areas to explore spatial variability.

Table 4. Comparison of global (OLS) and local spatial (GWR) regression diagnostics.

Overall (n = 66,543)				
	OLS		GWR	
Variables	Coeff	p-value	Min	Max
Intercept	−0.498	0.000	−2.602	1.388
Socioeconomic Disadvantage	−0.099	0.000	−1.035	0.428
Elderly and Disability	0.258	0.000	−0.588	1.112
Housing Density and Vehicle Access	−0.287	0.000	−2.423	0.763
Youth and Mobile Housing	0.205	0.000	−0.795	1.502
Group Quarters and Unemployment	−0.009	0.022	−1.529	1.619
AICc	186,261.678		153,877.144	
R-squared	0.276		0.666	
Urban (n = 51,990)				
	OLS		GWR	
Variables	Coeff	p-value	Min	Max
Intercept	−0.68	0.000	−2.633	1.153
Socioeconomic Disadvantage	−0.068	0.000	−0.673	0.353
Elderly and Disability	0.254	0.000	−0.61	1.148
Housing Density and Vehicle Access	−0.228	0.000	−1.558	0.782
Youth and Mobile Housing	0.133	0.000	−0.785	1.179
Group Quarters and Unemployment	0.008	0.056	−1.25	1.335
AICc	141,489.392		122,807.785	
R-squared	0.219		0.589	
Rural (n = 14,553)				
	OLS		GWR	
Variables	Coeff	p-value	Min	Max
Intercept	0.099	0.009	−1.034	1.329
Socioeconomic Disadvantage	−0.158	0.004	−0.778	0.364
Elderly and Disability	0.097	0.006	−0.483	0.75
Housing Density and Vehicle Access	−0.431	0.009	−1.169	0.341
Youth and Mobility	0.077	0.009	−0.672	1.001
Group Quarters and Unemployment	−0.042	0.007	−1.258	0.906
AICc	35,232.112		31,232.905	
R-squared	0.236		0.552	

3.2.1. The Overall Model

The OLS model for the overall dataset (n = 66,543) provides a broad understanding with an R^2 value of 0.276 (Figure 7a) and an AICc of 186,261.678, indicating that while the model captures some variability, it remains unexplained. In contrast, the GWR model significantly improves the explanatory power with an R^2 of 0.666 and a lower AICc of 153,877.144, underscoring the value of a localized approach in capturing the nuances of social vulnerability and flood risk. The coefficients for Socioeconomic Disadvantage, Elderly and Disability, Housing Density, Youth and Mobile Housing, and Group Quarters span a broad range, indicating different levels of impact across regions. These variations suggest that each component's effect on flood risk can be quite different depending on local conditions. The result for the overall model from Table 4 is visualized in Figure 7, showcasing the distribution of coefficients for each variable.

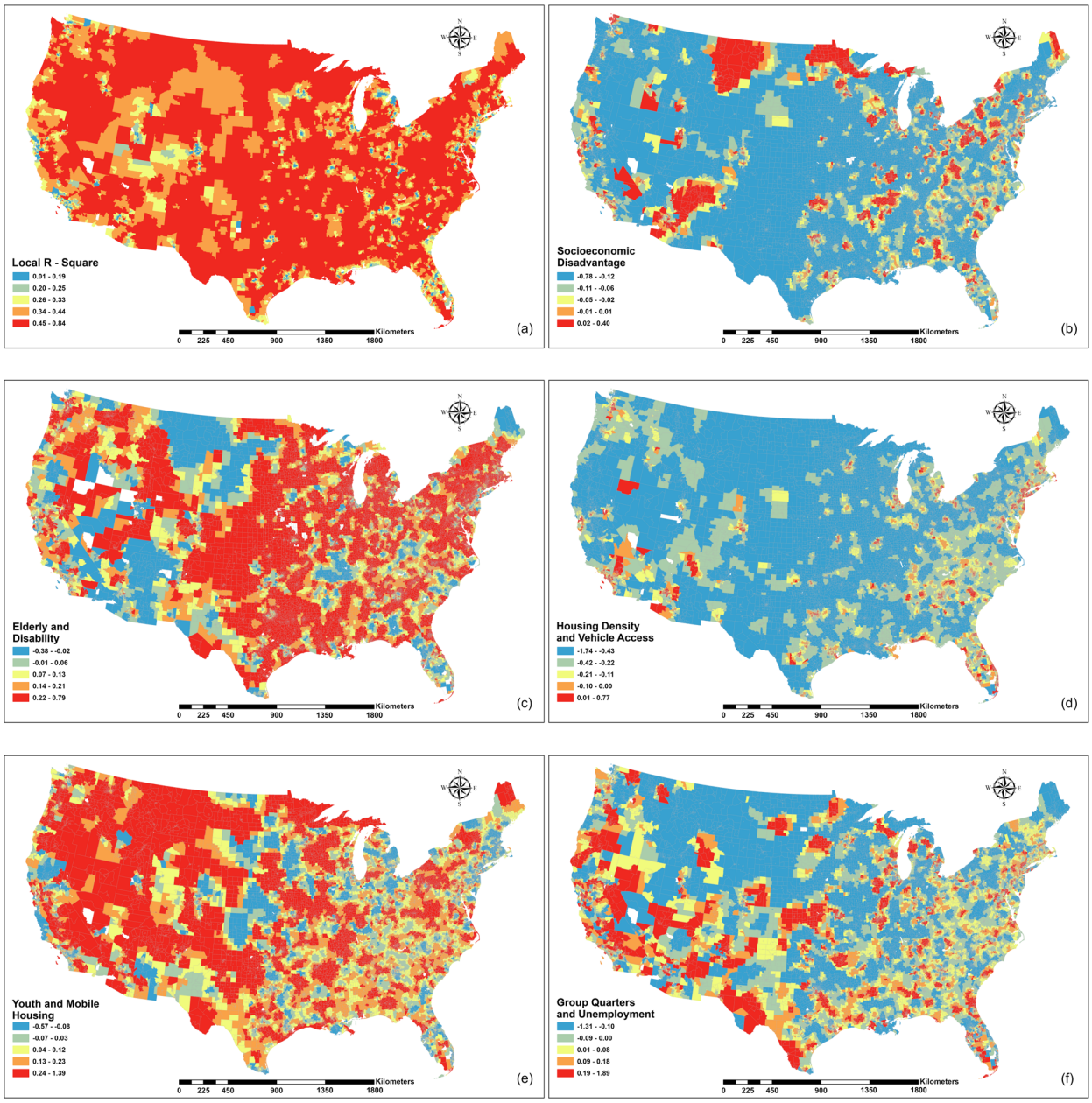


Figure 7. (**a**) R-squared distribution from GWR model and coefficients of (**b**) Socioeconomic Disadvantage, (**c**) Elderly and Disability, (**d**) Housing Density and Vehicle Access, (**e**) Youth and Mobile Housing, and (**f**) Group Quarters and Unemployment for the overall dataset.

3.2.2. Urban–Rural Differences

We conducted separate regression analyses for urban and rural census tracts to explore potential differences in the relationship between social vulnerability and flood risk. The results reveal distinct patterns between urban and rural areas, suggesting that these differences may reflect underlying spatial variability. Although the models did not show significant improvements, the variations in results showcase the importance of considering geographic context when analyzing social vulnerability and flood risk (Table 4).

In urban areas, the coefficients for Socioeconomic Disadvantage are tightly clustered around zero with a slight positive skew, indicating a modest positive correlation with flood risk (Figure 8a). Conversely, rural areas show a broader distribution of negative coefficients, suggesting an inverse relationship in these settings. Elderly and Disability coefficients reveal a similar pattern for both urban and rural areas, with rural areas showing a slightly

higher positive values (Figure 8b), indicating a stronger correlation with flood risk in rural zones than in urban areas. The Housing Density and Vehicle Access component shows a weak inverse relationship in urban areas (Figure 8c), likely reflecting the benefits of better infrastructure, while rural areas exhibit a stronger negative correlation. For Youth and Mobile Housing (Figure 8d), urban areas have a varied correlation with flood risk from high negative to high positive values, whereas rural areas show a slightly higher positive but varied relationship. Finally, Group Quarters and Unemployment (Figure 8e) in urban areas show a pronounced positive skew, highlighting a stronger correlation with flood risk, while rural areas display a more varied and generally negative association.

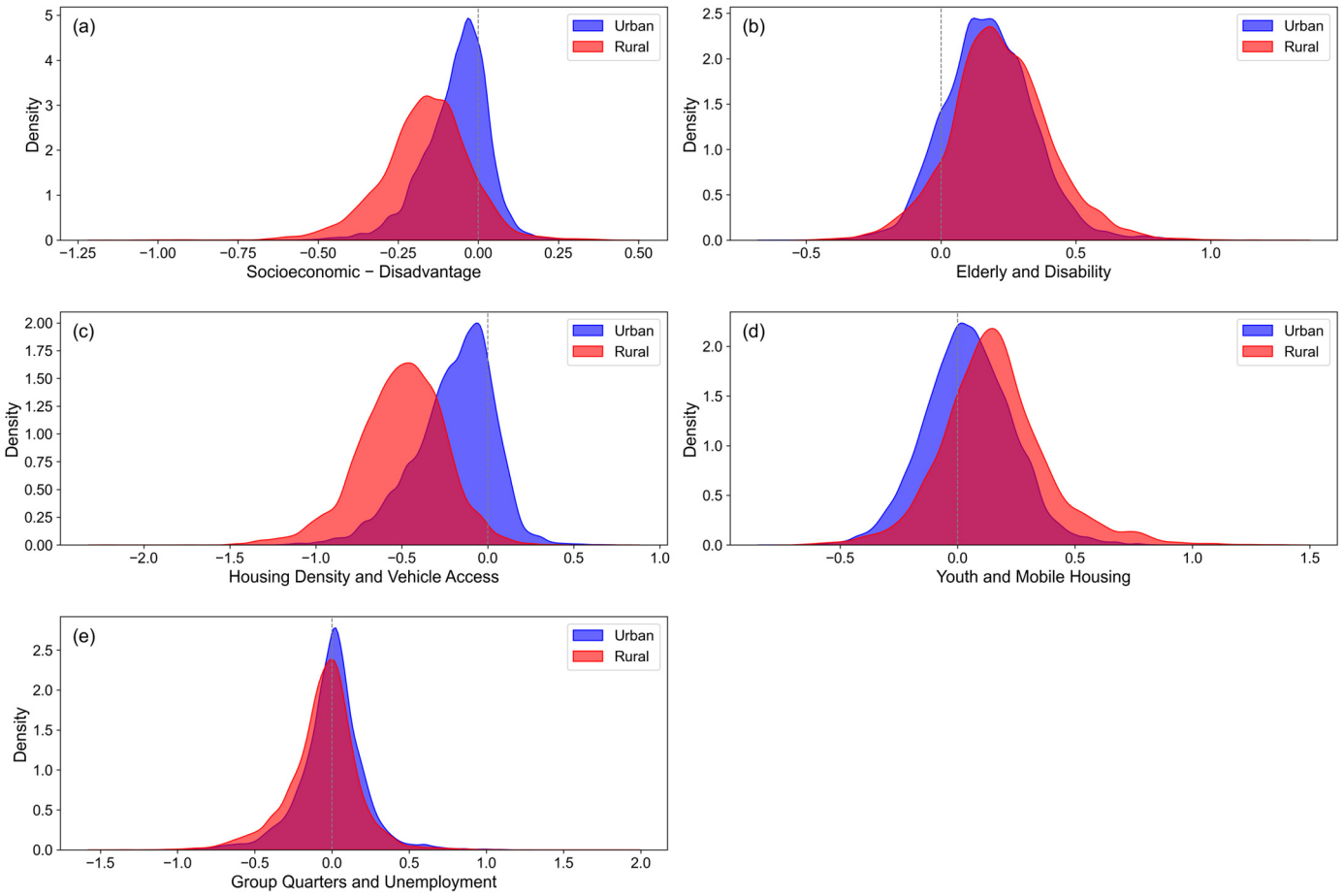


Figure 8. Coefficient distributions of social vulnerability components across urban and rural areas from GWR analysis of overall dataset. (**a**) Socioeconomic Disadvantage, (**b**) Elderly and Disability, (**c**) Housing Density and Vehicle Access, (**d**) Youth and Mobile Housing, and (**e**) Group Quarters and Unemployment.

The analysis of the top positive and negative coefficient values across urban and rural areas reveals distinct patterns for each social vulnerability component. Socioeconomic Disadvantage in urban areas shows a concentrated distribution of higher positive values, indicating a stronger positive correlation with flood risk, while rural areas exhibit a broader range with weaker associations (Figure 9a). The negative values suggest a weaker inverse relationship in urban areas compared to stronger negative correlations in rural settings (Figure 9b). Similarly, as shown in Figure 9c,d, Elderly and Disability components in urban regions tend to have higher positive coefficients, indicating a more pronounced link with flood risk, whereas rural areas display a wider and less consistent distribution, with the negative coefficients reflecting a weaker inverse relationship in urban areas and slightly stronger correlations in rural ones. The Housing Density and Vehicle Access component

follows this trend, with urban areas displaying higher positive values and a stronger relationship with flood risk, while rural areas show a more dispersed distribution and stronger negative associations (Figure 9e,f). For Youth and Mobile Housing, rural areas show varied but higher positive values, suggesting a stronger correlation with flood risk, while urban areas are less varied and less consistent, with negative coefficients indicating a weaker inverse relationship in rural settings and stronger negative associations in urban areas (Figure 9g,h). Finally, as shown in Figure 9i,j, Group Quarters and Unemployment components show that urban areas are characterized by higher positive values, reflecting a stronger correlation with flood risk, whereas rural areas have a broader distribution with weaker positive associations, and the negative coefficients reinforce this pattern, with urban areas showing weaker negative relationships and rural areas stronger negative correlations.

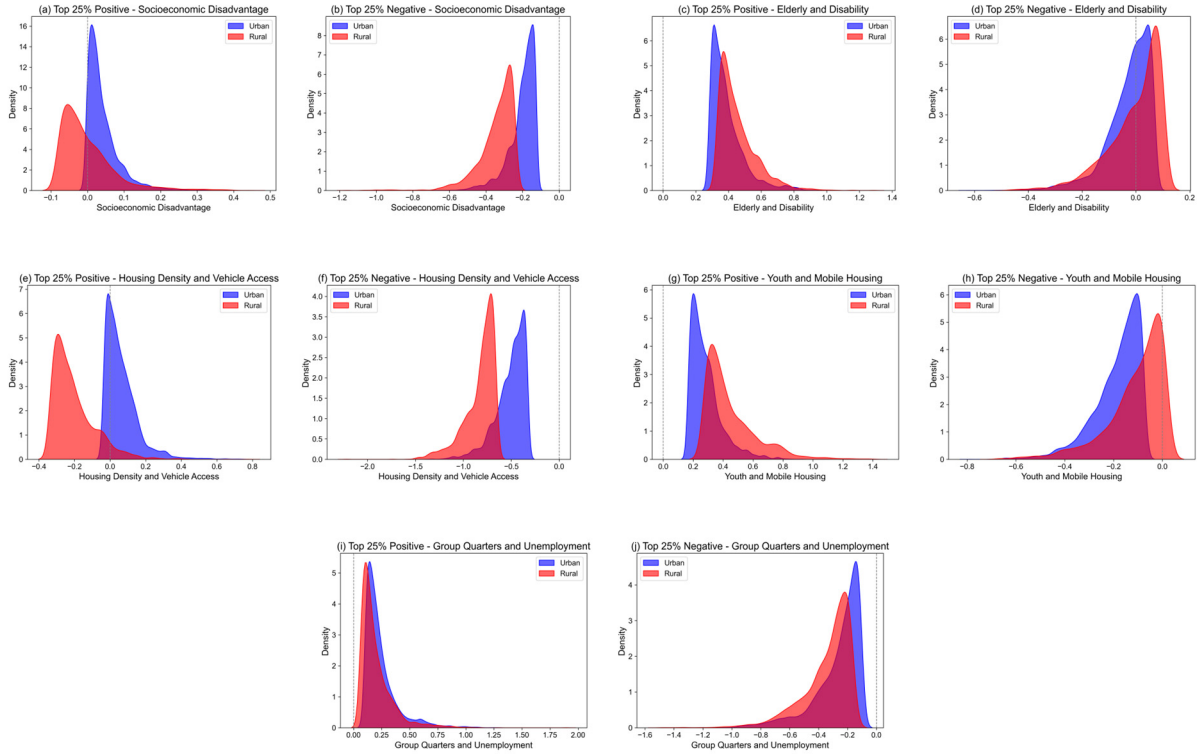


Figure 9. Distribution of top positive and negative coefficient values for social vulnerability components in urban and rural areas. (**a**,**b**) Socioeconomic Disadvantage, (**c**,**d**) Elderly and Disability, (**e**,**f**) Housing Density and Vehicle Access, (**g**,**h**) Youth and Mobile Housing, and (**i**,**j**) Group Quarters and Unemployment.

4. Discussion and Conclusions

In this comprehensive study involving 66,543 census tracts across the CONUS, we identified a significant relationship between social vulnerability and flood risk, validating the theory that communities with high social vulnerabilities face increased flood risks. Using global and local analyses, our investigation into different components of the SVI revealed more intricate associations between community vulnerabilities and flood risk than previously recognized. These findings align with literature suggesting that socioeconomically disadvantaged communities often face disproportionately high flood risks [10,15].

Cluster analysis highlighted distinct patterns of vulnerability and risk across urban and rural areas. Urban regions, particularly coastal areas, show high–high clusters of both vulnerability and flood risk, whereas rural areas, despite having lower population density, exhibit significant vulnerabilities due to inadequate infrastructure and resources [14]. This disparity underscores environmental justice issues, as rural communities often receive less attention in disaster preparedness and mitigation planning [11]. Urban centers, despite having more resources, also face significant challenges in managing and mitigating flood risks.

Our findings indicate that while urban areas have more vulnerable tracts in absolute terms, rural areas exhibit a higher ratio of vulnerability, emphasizing the need for targeted interventions in both contexts. These results align with broader environmental equity studies, which reveal that environmental hazards such as noise and air pollution disproportionately affect low-income and minority communities [10,39–44]. This reinforces the importance of region-specific strategies to address the unique vulnerabilities and needs of both urban and rural communities, ultimately promoting greater resilience and environmental justice.

Our study utilized Geographically Weighted Regression (GWR) to reveal the complex interplay between flood risk and social vulnerability across 66,543 census tracts in the CONUS. By employing GWR, we uncovered significant spatial variations in how social vulnerability components interact with flood risk, demonstrating the inadequacy of a uniform approach. For instance, urban areas exhibit higher concentrations of vulnerability related to poverty, people living in group quarters, dense housing, and unemployment, which underscores the need for targeted economic, social, and infrastructure interventions in these regions [7,37]. In contrast, rural areas, despite lower absolute numbers, show pronounced vulnerabilities due to socioeconomic disadvantages, disability, youths and mobile housing, and limited resources [14]. The analysis revealed that while urban areas face acute challenges in managing high absolute vulnerability, rural areas suffer from a higher vulnerability ratio with respect to specific factors like elderly care and youth needs [45].

The GWR analysis highlighted distinct needs across different SVI categories. For example, rural areas demonstrated a higher coefficient for Youth and Mobile Housing vulnerabilities, suggesting a greater potential impact from floods compared to urban areas where these issues are less pronounced. Conversely, the vulnerability associated with Elderly and Disability as well as Group Quarters and Unemployment showed similar impacts across both urban and rural settings, indicating that these factors uniformly affect flood risk irrespective of the geographic context [22]. This nuanced understanding emphasizes the necessity for differentiated strategies: urban areas require comprehensive interventions focused on social services, infrastructure and housing, and economic support, while rural areas need targeted efforts addressing socio-demographic disadvantages and resource limitations. Future studies should build on these findings by incorporating dynamic flood risk models and primary data collection to enhance our understanding of local vulnerabilities and improve flood risk management strategies [7,45].

The results of this study are valuable for policymakers, urban planners, and disaster management professionals. By identifying specific vulnerabilities and correlating them with flood risk, the findings can guide targeted interventions and resource allocation. This approach ensures that resources are directed to areas with the most acute needs, improving community resilience and preparedness. Additionally, this study's insights can inform future research and policy decisions, contributing to more effective flood risk management and advancing environmental justice. This research also sets a precedent for refining flood risk models and understanding vulnerability disparities more deeply. By incorporating a detailed spatial analysis and considering the local context, future studies can enhance flood risk management and support equitable environmental policies.

Despite the comprehensive nature of this study, several limitations must be acknowledged. Firstly, the analysis is constrained by the availability and quality of flood data. Incomplete or outdated flood records can impact the accuracy of flood risk assessments and the robustness of our findings. Additionally, while this study utilized the GWR model to capture spatial variability, it did not incorporate advanced techniques such as the MGWR, which could offer even finer resolution insights into the interplay between social vulnerability and flood risk. Furthermore, while analyzing floods in varying topography, it is important to take into consideration the relief which might be contributing to negative spatial autocorrelation, which may influence flood risk distribution and the spatial patterns of social vulnerability. Future research should address these limitations by incorporating more granular and dynamic flood data, exploring additional modeling techniques, and examin-

ing the impact of topographical factors to provide a more comprehensive understanding of the spatial dynamics of flood risk and social vulnerability.

Author Contributions: Conceptualization, Weibo Liu and Bishal Dhungana; methodology, Weibo Liu and Bishal Dhungana; formal analysis, Bishal Dhungana and Weibo Liu; writing—original draft preparation, Bishal Dhungana; writing—review and editing, Weibo Liu; supervision, Weibo Liu. All authors have read and agreed to the published version of the manuscript.

Funding: This research received no external funding.

Data Availability Statement: The original data presented in the study are openly available at the following links: CDC/ATSDR Social Vulnerability Index (SVI): https://www.atsdr.cdc.gov/placeandhealth/svi/data_documentation_download.html (accessed on 15 September 2023). EPA EnviroAtlas: https://www.epa.gov/enviroatlas/enviroatlas-interactive-map (accessed on 15 September 2023). Census Tract Relationship Files: https://www.census.gov/geographies/reference-files/time-series/geo/relationship-files.2020.html (accessed on 15 September 2023).

Acknowledgments: We would like to thank the three anonymous reviewers and editors for providing their valuable comments and suggestions which helped improve the manuscript greatly. We also thank the Florida Atlantic University School of Environmental, Coastal, and Ocean Sustainability for providing publication support.

Conflicts of Interest: The authors declare no conflicts of interest.

References

1. United Nations International Strategy for Disaster Reduction (UNISDR). *Global Assessment Report on Disaster Risk Reduction*; United Nations International Strategy for Disaster Reduction (UNISDR): Geneva, Switzerland, 2013.
2. Swain, D.L.; Langenbrunner, B.; Neelin, J.D.; Hall, A. Increasing precipitation volatility in twenty-first-century California. *Nat. Clim. Change* **2018**, *8*, 427–433. [CrossRef]
3. USGS Fact Sheet 2006–3026: Flood Hazards—A National Threat. 2006. Available online: https://pubs.usgs.gov/fs/2006/3026/ (accessed on 15 September 2023).
4. Chen, X.; Zhang, H.; Chen, W.; Huang, G. Urbanization and climate change impacts on future flood risk in the Pearl River Delta under shared socioeconomic pathways. *Sci. Total Environ.* **2021**, *762*, 143144. [CrossRef]
5. Wing, O.E.; Bates, P.D.; Smith, A.M.; Sampson, C.C.; Johnson, K.A.; Fargione, J.; Morefield, P. Estimates of present and future flood risk in the conterminous United States. *Environ. Res. Lett.* **2018**, *13*, 034023. [CrossRef]
6. FEMA's National Preparedness Report Underscores Continued Threat of Climate Change. FEMA.gov. 2022. Available online: https://www.fema.gov/press-release/20221229/femas-national-preparedness-report-underscores-continued-threat-climate (accessed on 15 September 2023).
7. Cutter, S.L.; Boruff, B.J.; Shirley, W.L. Social vulnerability to environmental hazards. *Soc. Sci. Q.* **2003**, *84*, 242–261. [CrossRef]
8. Singh, S.R.; Eghdami, M.R.; Singh, S. The concept of social vulnerability: A review from disasters perspectives. *Int. J. Interdiscip. Multidiscip. Stud.* **2014**, *1*, 71–82.
9. Flanagan, B.E.; Gregory, E.W.; Hallisey, E.J.; Heitgerd, J.L.; Lewis, B. A social vulnerability index for disaster management. *J. Homel. Secur. Emerg. Manag.* **2011**, *8*. [CrossRef]
10. Chakraborty, L.; Rus, H.; Henstra, D.; Thistlethwaite, J.; Minano, A.; Scott, D. Exploring spatial heterogeneity and environmental injustices in exposure to flood hazards using geographically weighted regression. *Environ. Res.* **2022**, *210*, 112982. [CrossRef]
11. Brulle, R.J.; Pellow, D.N. Environmental justice: Human health and environmental inequalities. *Annu. Rev. Public Health* **2006**, *27*, 103–124. [CrossRef]
12. Adger, W.N. Vulnerability. *Glob. Environ. Change* **2006**, *16*, 268–281. [CrossRef]
13. Qiang, Y. Disparities of population exposed to flood hazards in the United States. *J. Environ. Manag.* **2019**, *232*, 295–304. [CrossRef]
14. Tate, E.; Rahman, M.A.; Emrich, C.T.; Sampson, C.C. Flood exposure and social vulnerability in the United States. *Nat. Hazards* **2021**, *106*, 435–457. [CrossRef]
15. Collins, T.W.; Grineski, S.E.; Chakraborty, J.; Flores, A.B. Environmental injustice and Hurricane Harvey: A household-level study of socially disparate flood exposures in Greater Houston, Texas, USA. *Environ. Res.* **2019**, *179 Pt A*, 108772. [CrossRef]
16. Chakraborty, L.; Thistlethwaite, J.; Scott, D.; Henstra, D.; Minano, A.; Rus, H. Assessing social vulnerability and identifying spatial hotspots of flood risk to inform socially just flood management policy. *Risk Anal.* **2023**, *43*, 1058–1078. [CrossRef] [PubMed]
17. Maantay, J.; Maroko, A. Mapping Urban Risk: Flood Hazards, Race, & Environmental Justice in New York. *Appl. Geogr.* **2009**, *29*, 111–124. [CrossRef]
18. Chakraborty, L.; Thistlethwaite, J.; Minano, A.; Henstra, D.; Scott, D. Leveraging Hazard, Exposure, and Social Vulnerability Data to Assess Flood Risk to Indigenous Communities in Canada. *Int. J. Disaster Risk Sci.* **2021**, *12*, 821–838. [CrossRef]
19. Qiang, Y.; Lam, N.S.N.; Cai, H.; Zou, L. Changes in Exposure to Flood Hazards in the United States. *Ann. Am. Assoc. Geogr.* **2017**, *107*, 1332–1350. [CrossRef]

20. Collins, T.W.; Grineski, S.E.; Chakraborty, J. Environmental injustice and flood risk: A conceptual model and case comparison of metropolitan Miami and Houston, USA. *Reg. Environ. Chang.* **2018**, *18*, 311–323. [CrossRef] [PubMed]
21. Connor, A. When It Rains, It Floods: A Socio-Spatial Flood Vulnerability Analysis of Alexandria, Virginia. 2023. Available online: https://ecommons.cornell.edu/items/faccef84-fe25-4df0-897d-3a4887d7261b (accessed on 15 September 2023).
22. Montgomery, M.C.; Chakraborty, J. Assessing the environmental justice consequences of flood risk: A case study in Miami, Florida. *Environ. Res. Lett.* **2015**, *10*, 095010. [CrossRef]
23. Jamshed, A.; Birkmann, J.; Feldmeyer, D.; Rana, I.A. A conceptual framework to understand the dynamics of rural-urban linkages for rural flood vulnerability. *Sustainability* **2020**, *12*, 2894. [CrossRef]
24. Tyler, J.; Entress, R.M.; Sun, P.; Noonan, D.; Sadiq, A.A. Is flood mitigation funding distributed equitably? Evidence from coastal states in the southeastern United States. *J. Flood Risk Manag.* **2023**, *16*, e12886. [CrossRef]
25. Tascón-González, L.; Ferrer-Julià, M.; Ruiz, M.; García-Meléndez, E. Social vulnerability assessment for flood risk analysis. *Water* **2020**, *12*, 558. [CrossRef]
26. Rehman, S.; Sahana, M.; Hong, H.; Sajjad, H.; Ahmed, B.B. A systematic review on approaches and methods used for flood vulnerability assessment: Framework for future research. *Nat. Hazards* **2019**, *96*, 975–998. [CrossRef]
27. Moreira, L.L.; de Brito, M.M.; Kobiyama, M. Effects of different normalization, aggregation, and classification methods on the construction of flood vulnerability indexes. *Water* **2021**, *13*, 98. [CrossRef]
28. Woznicki, S.A.; Baynes, J.; Panlasigui, S.; Mehaffey, M.; Neale, A. Development of a spatially complete floodplain map of the conterminous United States using random forest. *Sci. Total Environ.* **2019**, *647*, 942–953. [CrossRef]
29. USDA ERS—Rural-Urban Commuting Area Codes. 2023. Available online: https://www.ers.usda.gov/dataproducts/rural-urban-commuting-area-codes (accessed on 15 September 2023).
30. USDA ERS—Documentation. 2023. Available online: https://www.ers.usda.gov/data-products/rural-urbancommuting-area-codes/documentation/ (accessed on 15 September 2023).
31. US Census Bureau. Relationship Files. 2023. Available online: https://www.census.gov/geographies/reference-files/time-series/geo/relationshipfiles.2020.html (accessed on 15 September 2023).
32. Pedregosa, F.; Varoquaux, G.; Gramfort, A.; Michel, V.; Thirion, B.; Grisel, O.; Blondel, M.; Prettenhofer, P.; Weiss, R.; Dubourg, V.; et al. Scikit-learn: Machine Learning in Python. *J. Mach. Learn. Res.* **2011**, *12*, 2825–2830. [CrossRef]
33. Kaiser, H.F. The application of electronic computers to factor analysis. *Educ. Psychol. Meas.* **1960**, *20*, 141–151. [CrossRef]
34. Yoon, D.K. Assessment of social vulnerability to natural disasters: A comparative study. *Natural Hazards.* **2012**, *63*, 823–843. [CrossRef]
35. Huang, Q.; Jackson, S.; Derakhshan, S.; Lee, L.; Pham, E.; Jackson, A.; Cutter, S.L. Urban-rural differences in COVID-19 exposures and outcomes in the South: A preliminary analysis of South Carolina. *PLoS ONE* **2021**, *16*, e0246548. [CrossRef] [PubMed]
36. Anselin, L. Local Indicators of Spatial Association—LISA. *Geogr. Anal.* **1995**, *27*, 93–115. [CrossRef]
37. Fotheringham, A.S.; Brunsdon, C.; Charlton, M.E. Geographically weighted regression. *Sage Handb. Spat. Anal.* **2009**, *1*, 243–254. [CrossRef]
38. Oshan, T.M.; Li, Z.; Kang, W.; Wolf, L.J.; Fotheringham, A.S. mgwr: A Python implementation of multiscale geographically weighted regression for investigating process spatial heterogeneity and scale. *ISPRS Int. J. Geo-Inf.* **2019**, *8*, 269. [CrossRef]
39. Buzzelli, M.; Jerrett, M. Geographies of Susceptibility and Exposure in the City: Environmental Inequity of Traffic-Related Air Pollution in Toronto. *Can. J. Reg. Sci.* **2006**, *30*, 195–210.
40. Carrier, M.; Apparicio, P.; Séguin, A.M. Road traffic noise in Montreal and environmental equity: What is the situation for the most vulnerable population groups? *J. Transp. Geogr.* **2016**, *51*, 1–8. [CrossRef]
41. Crouse, D.L.; Ross, N.A.; Goldberg, M.S. Double burden of deprivation and high concentrations of ambient air pollution at the neighbourhood scale in Montreal, Canada. *Soc. Sci. Med. (1982)* **2009**, *69*, 971–981. [CrossRef] [PubMed]
42. Dale, L.M.; Goudreau, S.; Perron, S.; Ragettli, M.S.; Hatzopoulou, M.; Smargiassi, A. Socioeconomic status and environmental noise exposure in Montreal, Canada. *BMC Public Health* **2015**, *15*, 205. [CrossRef]
43. Pinault, L.; Crouse, D.; Jerrett, M.; Brauer, M.; Tjepkema, M. Spatial associations between socioeconomic groups and NO_2 air pollution exposure within three large Canadian cities. *Environ. Res.* **2016**, *147*, 373–382. [CrossRef]
44. Tooke, T.R.; Klinkenberg, B.; Coops, N.C. A geographical approach to identifying vegetation-related environmental equity in Canadian cities. *Environ. Plan. B Plan. Des.* **2010**, *37*, 1040–1056. [CrossRef]
45. Holifield, R.; Porter, M.; Walker, G. Spaces of environmental justice: Frameworks for critical engagement. *Antipode* **2009**, *41*, 591–612. [CrossRef]

Disclaimer/Publisher's Note: The statements, opinions and data contained in all publications are solely those of the individual author(s) and contributor(s) and not of MDPI and/or the editor(s). MDPI and/or the editor(s) disclaim responsibility for any injury to people or property resulting from any ideas, methods, instructions or products referred to in the content.